

Disruption of the endocytic protein HIP1 results in neurological deficits and decreased AMPA receptor trafficking

Martina Metzler, Bo Li¹, Lu Gan, John Georgiou², Claire-Anne Gutekunst³, Yushan Wang⁴, Enrique Torre³, Rebecca S.Devon, Rosemary Oh, Valerie Legendre-Guillemain⁵, Mark Rich³, Christine Alvarez, Marina Gertsenstein², Peter S.McPherson⁵, Andras Nagy², Yu Tian Wang⁴, John C.Roder², Lynn A.Raymond¹ and Michael R.Hayden⁶

Centre for Molecular Medicine and Therapeutics, Childrens and Womens Hospital, Department of Medical Genetics, University of British Columbia, Vancouver, BC, V5Z 4H4, ¹Kinsmen Laboratory, Department of Psychiatry and Brain Research Centre (BRC) and ⁴Department of Medicine and BRC, University of British Columbia, BC, V6T 1Z3, ²Samuel Lunenfeld Research Institute, Mount Sinai Hospital, Toronto, M5G 1X5, ³Department of Neurology and Neurosurgery, Montreal Neurological Institute, McGill University, Montreal, PQ, H3A 2B4, Canada and ⁵Emory University School of Medicine, Atlanta, GA 30322, USA

⁶Corresponding author
e-mail: mrh@cmmt.ubc.ca

Huntingtin interacting protein 1 (HIP1) is a recently identified component of clathrin-coated vesicles that plays a role in clathrin-mediated endocytosis. To explore the normal function of HIP1 *in vivo*, we created mice with targeted mutation in the HIP1 gene (HIP1^{-/-}). HIP1^{-/-} mice develop a neurological phenotype by 3 months of age manifest with a failure to thrive, tremor and a gait ataxia secondary to a rigid thoracolumbar kyphosis accompanied by decreased assembly of endocytic protein complexes on liposomal membranes. In primary hippocampal neurons, HIP1 colocalizes with GluR1-containing AMPA receptors and becomes concentrated in cell bodies following AMPA stimulation. Moreover, a profound dose-dependent defect in clathrin-mediated internalization of GluR1-containing AMPA receptors was observed in neurons from HIP1^{-/-} mice. Together, these data provide strong evidence that HIP1 regulates AMPA receptor trafficking in the central nervous system through its function in clathrin-mediated endocytosis.

Keywords: clathrin/endocytosis/glutamate receptors/Huntington's disease/synapse

Introduction

Clathrin-mediated endocytosis allows eukaryotic cells to respond to their environment by controlling membrane composition and the number of receptors, transporters and ion channels expressed on the cell surface (Buckley *et al.*, 2000; McPherson *et al.*, 2001). The principal steps in clathrin-mediated endocytosis involve the recruitment of clathrin to sites of endocytosis demarcated by the adaptor

complex AP2 (Ahle *et al.*, 1988). AP2 is a heterotetrameric adaptor protein that binds cargo and links clathrin to phospholipid-containing membranes. Through cooperation with other coat proteins, such as AP180 in neurons, AP2 drives the assembly of clathrin lattices and the formation of invaginated clathrin-coated pits (CCPs) (Hao *et al.*, 1999; Ford *et al.*, 2001). Once CCPs are formed, accessory proteins such as endophilin, amphiphysin, dynamin and synaptojanin influence the budding and detachment of clathrin-coated vesicles (CCVs) from the resident membrane, followed by loss of the clathrin coat, intracellular vesicle transport and subsequent fusion with target membranes (Brodsky *et al.*, 2001).

In neurons, clathrin-mediated endocytosis facilitates the rapid retrieval of synaptic vesicles at the presynaptic nerve terminal and is functionally coupled with synaptic vesicle exocytosis (De Camilli *et al.*, 2001; Sun *et al.*, 2002). In the postsynaptic compartment, clathrin-mediated endocytosis regulates the surface expression of glutamate receptors in excitatory synapses in the brain (Roche *et al.*, 2001; Sheng and Kim, 2002). In particular, AMPA (α -amino-3-hydroxy-5-methyl-4-isoxazolepropionic acid)-type glutamate receptors are dynamic and targets of constitutive and regulated clathrin-mediated endocytosis (Carroll *et al.*, 1999; Lin *et al.*, 2000; Man *et al.*, 2000). AMPA receptors are multimeric proteins composed of the subunit GluR1 to GluR4 containing a short (GluR2 and GluR3) or long (GluR1 and GluR4) cytoplasmic tail, which determines the trafficking characteristics through interaction with unique sets of proteins (Lee *et al.*, 2002; Malinow and Malenka, 2002).

We and others have recently identified and characterized a novel endocytic protein, huntingtin interacting protein 1 (HIP1) (Kalchman *et al.*, 1997; Metzler *et al.*, 2001; Waelter *et al.*, 2001). HIP1 colocalizes with AP2 and clathrin in various cells and is a component of CCVs isolated from brain extracts. HIP1 binds directly to AP2, clathrin heavy chain (CHC) and clathrin light chain (CLC) and assembles clathrin through its coiled-coil domain *in vitro* (Legendre-Guillemain *et al.*, 2002). Overexpression of small fragments encompassing binding sites for AP2 and clathrin act as dominant-negative mutants and inhibit transferrin uptake in COS7 cells. In addition, HIP1 contains a phosphatidylinositol-4,5-bisphosphate [Ptd-Ins(4,5)P₂]-binding motif that is present in its ANTH (AP180 N-terminal Homology) domain (Ford *et al.*, 2001, 2002; Itoh *et al.*, 2001), which is structurally related to the ENTH (Epsin N-terminal Homology) domain of epsin that also binds to Ptd-Ins(4,5)P₂ and plays a critical role in clathrin-mediated endocytosis (Rosenthal *et al.*, 1999). The combination of Ptd-Ins(4,5)P₂ interaction, together with clathrin and AP2 binding sites and the ability to polymerize clathrin is a property of HIP1 shared with a growing list of endocytic proteins including AP180 and

epsin (Ford *et al.*, 2001, 2002; Itoh *et al.*, 2001). Each of these linker proteins can, either alone or in cooperation with AP2, attract clathrin to phospholipid-containing membranes to stimulate clathrin assembly and to further enhance AP2-dependent coat formation *in vivo* (Ford *et al.*, 2001). HIP1, like AP2 and AP-180, may be involved in cargo selection allowing for greater control of the proteins and lipids undergoing endocytosis.

HIP1 was identified through its interaction with huntingtin, the polyglutamine-containing protein that causes Huntington's disease (HD) (Kalchman *et al.*, 1997; Wanker *et al.*, 1997). HD is a progressive neuropsychiatric illness associated with selective neuronal loss caused by polyglutamine expansion in huntingtin. The expanded allele leads to a decreased interaction between huntingtin and HIP1, and alters the interaction with several other huntingtin-associating proteins involved in intracellular transport (Li *et al.*, 1995; Kalchman *et al.*, 1997; Faber *et al.*, 1998). Interestingly, huntingtin itself is likely to play a role in intracellular trafficking as it associates with transport vesicles and microtubules and interacts with the α -adaptin C subunit of the AP2 complex and endophilin A3 (SH3GL3) (DiFiglia *et al.*, 1995; Faber *et al.*, 1998; Sittler *et al.*, 1998).

To gain insight into the normal function of HIP1 *in vivo* and to identify potential targets whose activity is influenced by HIP1, we have created mice with targeted disruption of HIP1 (HIP1^{-/-}). These mice are viable and develop a neurological phenotype characterized by

wasting, and an abnormal gait secondary to a thoracolumbar kyphosis, accompanied by a defect in AMPA receptor trafficking, demonstrating an essential role of HIP1 in the central nervous system (CNS) and the identification of AMPA receptors as targets of HIP1 endocytic function.

Results

Targeted disruption of the HIP1 gene

A promoter-trap gene-targeting strategy was applied to inactivate the HIP1 gene whose expression was confirmed in mouse embryonic stem (ES) cells by RT-PCR. The promoter-trap vector pIFS contains an SA-IRES- β Geo-pA cassette encoding a bifunctional *lacZ*-neomycin fusion protein, which was used to replace exon 8 and adjacent intronic sequences to inactivate both HIP1 isoforms that result from alternative splicing at the 5'-end of HIP1 transcript (Figure 1A; Supplementary data 1, available at *The EMBO Journal Online*; Chopra *et al.*, 2000). Five homologous recombinant ES cell clones were identified and characterized by genomic Southern blot analyses to generate mice heterozygous for this targeted mutation (Supplementary data 1). The genotype of newborns derived from heterozygous matings of three independent lines corresponded to a normal Mendelian distribution demonstrating that HIP1^{-/-} mice are viable. HIP1 expression in cortical and striatal tissue was completely lacking (Figure 1B)

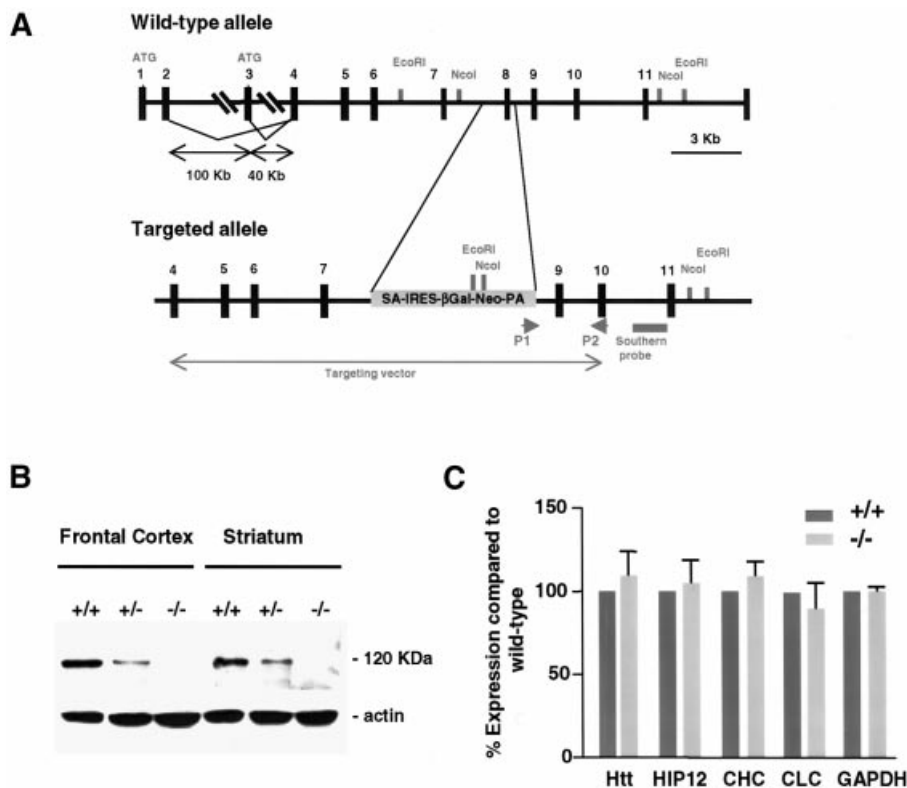


Fig. 1. Generation of HIP1^{-/-} mice that lack HIP1. (A) Schematic presentation of the HIP1 locus and the targeted allele. The closed arrow indicates the region that corresponds to the targeting vector. P1 and P2 indicate the location of primers that were used to identify homologous recombinant ES cell clones by PCR. (B) Lack of HIP1 expression in HIP1^{-/-} mice is demonstrated by western blot analysis of tissues isolated from frontal cortex and striatum of wild-type (+/+), HIP1 (+/-) and HIP1 (-/-) mice. (C) Lack of HIP1 expression does not alter the expression level of HIP1 interacting proteins in brain lysates of adult wild-type (dark grey bars) and HIP1^{-/-} mice (light grey bars).

with normal expression of HIP1 interacting proteins (Figure 1C). Although HIP1 can heterodimerize with its family member HIP12, expression of HIP12 was normal (Legendre-Guillemain *et al.*, 2002).

During the first month after birth, HIP1^{-/-} mice were indistinguishable from heterozygous and wild-type littermates in appearance, size and body weight. Morphologic and histologic analysis revealed that major organs includ-

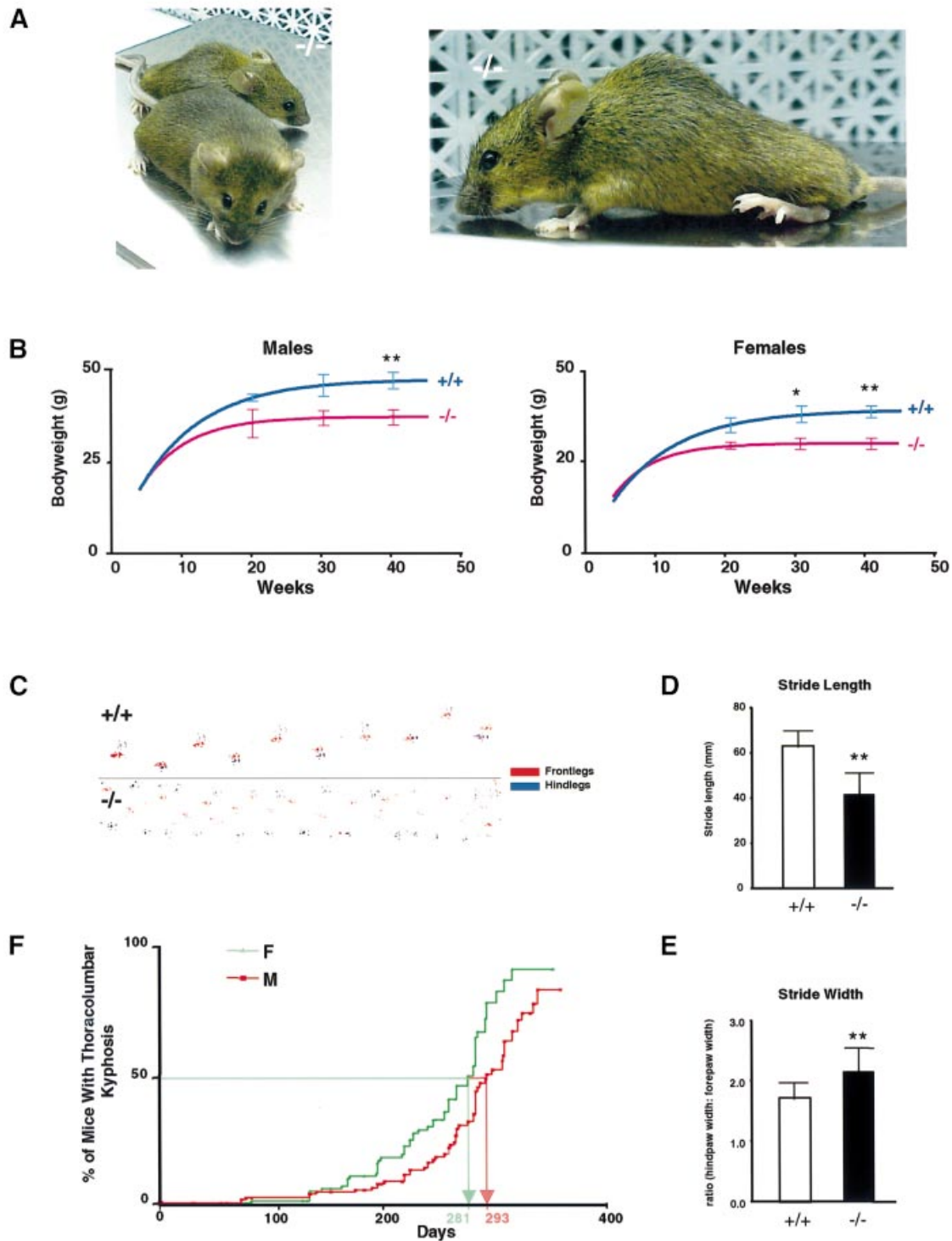


Fig. 2. HIP1^{-/-} mice develop a neurological phenotype. (A) A thoracolumbar kyphosis is evident in a 7-month-old HIP1^{-/-} mouse compared with its wild-type (+/+) littermate. (B) HIP1^{-/-} males ($n = 81$, left) and HIP1^{-/-} females ($n = 83$, right) exhibit a significant and sustained reduction in body weight in comparison with wild-type (+/+) males ($n = 65$, left) and wild-type (+/+) females ($n = 81$, right) 7–9 months after birth ($*P < 0.05$, $**P < 0.005$ by t -test). (C) HIP1^{-/-} mice with thoracolumbar kyphosis show gait abnormalities compared with wild-type (+/+) mice. (D) Stride length is significantly reduced in HIP1^{-/-} mice ($n = 13$) compared with wild type (+/+) ($n = 14$, $**P < 0.005$ by t -test). (E) Stride width is significantly increased in HIP1^{-/-} mice compared with wild type (+/+) ($**P < 0.005$ by t -test). (F) The percentage of male and female HIP1^{-/-} mice with thoracolumbar kyphosis is shown as a function of age. Females have a slightly earlier onset of the phenotype.

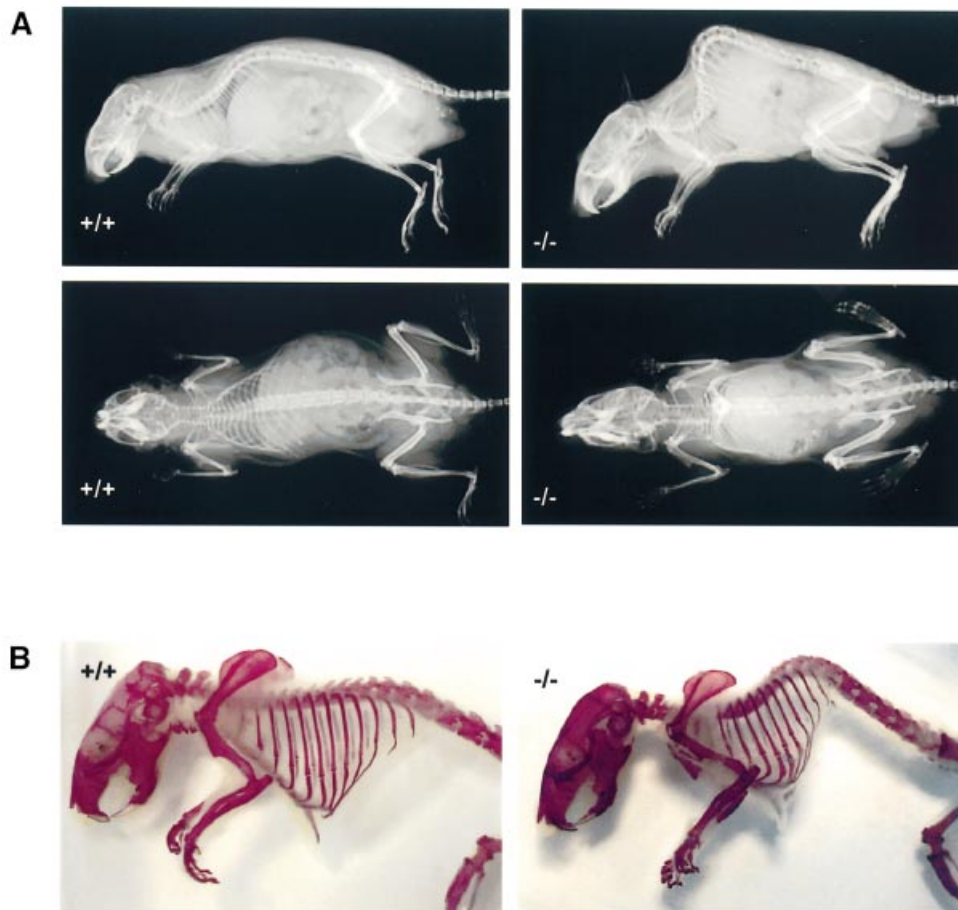


Fig. 3. The thoracolumbar kyphosis in HIP1^{-/-} mice does not result from a congenital skeletal defect or dysplasia. **(A)** The presence of a thoracolumbar kyphosis is evident in X-rays from a 7-month-old HIP1^{-/-} mouse in comparison with its wild-type (+/+) littermate. Both mice are shown in lateral (top) and anteroposterior (bottom) views. **(B)** No congenital skeletal defect or dysplasia is evident in Alizarin Red-stained skeletons prepared from a HIP1^{-/-} mouse at 7 months of age in comparison with its wild-type (+/+) littermate.

ing brain developed normally (data not shown). Interestingly, HIP1^{-/-} mice exhibit a defect in reproduction that is consistent with the expression of HIP1 in testes and ovaries (K.Khatchadourian, M.Metzler, C.E.Smith, M.Gregory, D.G.Cyr and L.Hermo, manuscript in preparation).

HIP1^{-/-} mice develop a progressive neurological phenotype

From ~12 weeks of age, HIP1^{-/-} mice show growth retardation and develop a progressive marked and rigid thoracolumbar kyphosis (Figure 2A and B). HIP1^{-/-} mice are less active and the dynamic range of motion in both their fore and hind limbs is markedly limited. HIP1^{-/-} mice have reduced muscle bulk and an abnormal gait characterized by a reduction in average stride length ($P < 0.001$) and wide splaying of the hindlegs resulting in an increase in stride width ($P = 0.004$; Figure 2C–E). HIP1^{-/-} mice also demonstrate a tremor that involves primarily the trunk musculature and which occurs frequently (>10 times per min) lasting less than 5 s. The phenotype is progressive and results in premature death several months after development of the thoracolumbar kyphosis.

A total of 159 male and 130 female mice were followed throughout their lifespan. Fifty per cent of mice develop the thoracolumbar kyphosis and neurological abnormal-

ities by 9–10 months of age with >85% demonstrating abnormalities by 1 year of age. Females are affected earlier than males ($P < 0.0012$; Figure 2F).

X-ray analyses on wild-type and homozygous littermates revealed no evidence of abnormal vertebral anatomy or bony deformity, joint destruction or malignment in the limbs of HIP1^{-/-} mice (Figure 3A). Moreover, examination of the prepared skeleton stained by Alizarin Red did not reveal any underlying congenital spinal anomalies or a generalized skeletal dysplasia (Figure 3B).

No sign of denervation or myopathy was detected by electromyography (EMG). Furthermore, a neuropathy or defects at the neuromuscular junction were ruled out by nerve conduction analyses. Compound muscle action potential (CMAP) amplitudes were recorded from the gastrocnemius muscle in the leg of 9-month-old HIP1^{-/-} mice and wild-type controls. In HIP1^{-/-} mice, the mean CMAP was 81.5 ± 13.4 mV compared with 91.6 ± 13.7 mV in control littermates ($n = 6$, 12 legs, mean \pm SD, $P = 0.09$). To determine whether defects in neuromuscular transmission were present, repetitive nerve stimulation was performed at 2 Hz. No decrement in CMAP amplitude with repetitive stimulation was present in HIP1^{-/-} mice (data not shown).

Taken together, these findings show that the phenotype in HIP1^{-/-} mice is not due to congenital skeletal deform-

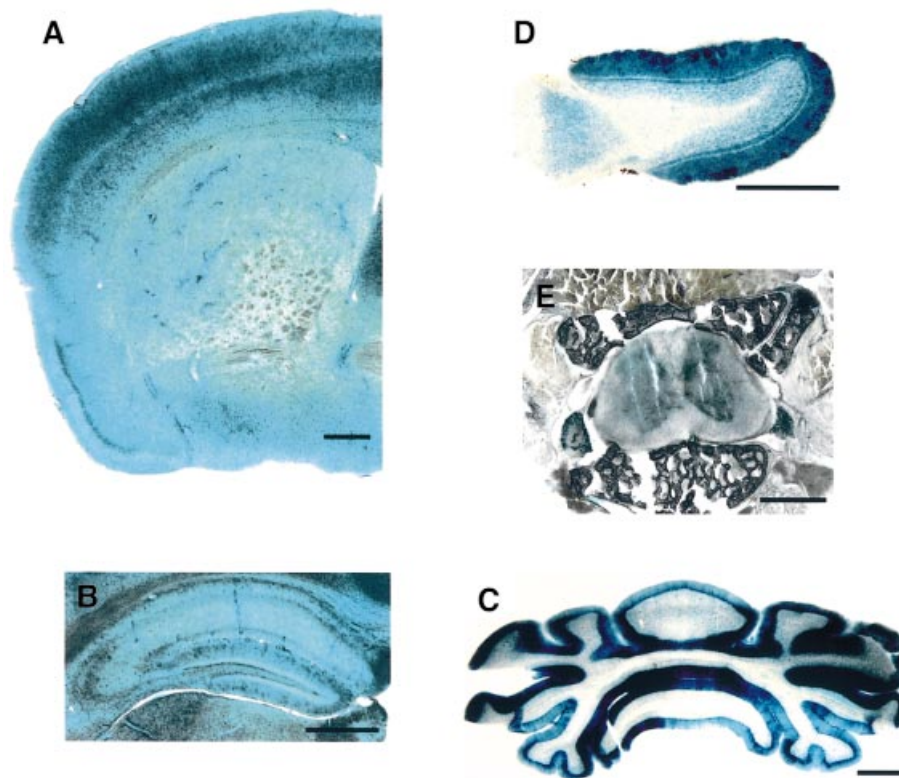


Fig. 4. HIP1 is expressed in adult brain and spinal cord. (A–E) HIP1 is expressed in coronal sections through the frontal cortex (A), the hippocampus (B), the cerebellum (C), the spinal cord (E) and in transverse sections through the olfactory bulb (D). Sections were prepared from 4-month-old $HIP1^{-/-}$ mice and analyzed by *lacZ* staining. Scale bar = 1 mm.

ities, dysplasia or primary defects in muscle or the peripheral nervous system. Based on this analysis we focused our attention on the role of HIP1 in the central nervous system.

HIP1 is expressed in brain and spinal cord and lack of HIP1 does not obviously affect brain morphology

Western blot analyses have shown that HIP1 expression is most abundant in brain with some expression in peripheral tissues and reproductive organs (Kalchman *et al.*, 1997; data not shown). *LacZ* expression analyses in $HIP1^{-/-}$ mice revealed that HIP1 is expressed in cortical tissue, in particular in the pyriform cortex, the hippocampus, the molecular layer of the cerebellum and the olfactory bulb (Figure 4A–D). However, gross brain morphology and measurements of cortical, hippocampal and striatal volumes, and hippocampal and striatal neuronal densities revealed no differences in $HIP1^{-/-}$ mice ($n = 2$; Figure 4; data not shown). High expression of HIP1 was also detected in the spinal cord with a greater abundance of HIP1 in gray than white matter (Figure 4E).

Binding of clathrin coat components is significantly diminished in brain extracts from $HIP1^{-/-}$ mice

HIP1 contains several protein motifs that suggest a linker function in endocytosis and intracellular transport (Figure 5A). HIP1 can bind to liposomal membranes enabling the recruitment of clathrin (Mishra *et al.*, 2001). This recruitment function of HIP1 and its potential role in

stabilizing protein complexes at the membrane was directly tested in liposomal binding experiments with brain lysates from E18 embryos that express large amounts of HIP1 but relatively low levels of HIP12. This strategy avoided functional redundancy between family members since both proteins share several endocytic properties, such as clathrin binding and assembly activity.

Quantitative analysis of protein recruitment to liposomal membranes revealed >40% reduction in attachment of all HIP1 interacting endocytic proteins, including HIP12, in tissue from $HIP1^{-/-}$ compared with wild-type embryos ($n = 3$, $P < 0.05$; Figure 5B and C). In particular, binding of the adaptor protein AP2 was reduced by >75% ($n = 3$, $P < 0.0005$; Figure 5C). This reduction did not result from alterations in expression of these proteins as no significant differences were apparent between wild-type and $HIP1^{-/-}$ littermates (Figure 5D). These results suggest that membrane attachment of endocytic proteins is diminished in $HIP1^{-/-}$ mice and that clathrin-mediated vesicle formation is likely to be impaired.

Because of this finding and the fact that HIP1 is expressed in primary neurons and colocalizes with clathrin and AP2 (Metzler *et al.*, 2001), we studied clathrin-dependent processes in primary neurons from $HIP1^{-/-}$ mice as additional measures of HIP1 function in clathrin-mediated endocytosis.

HIP1 is expressed in the somatodendritic compartment in neurons

Double immunofluorescence studies revealed that HIP1 immunostaining is diffuse throughout cell bodies and

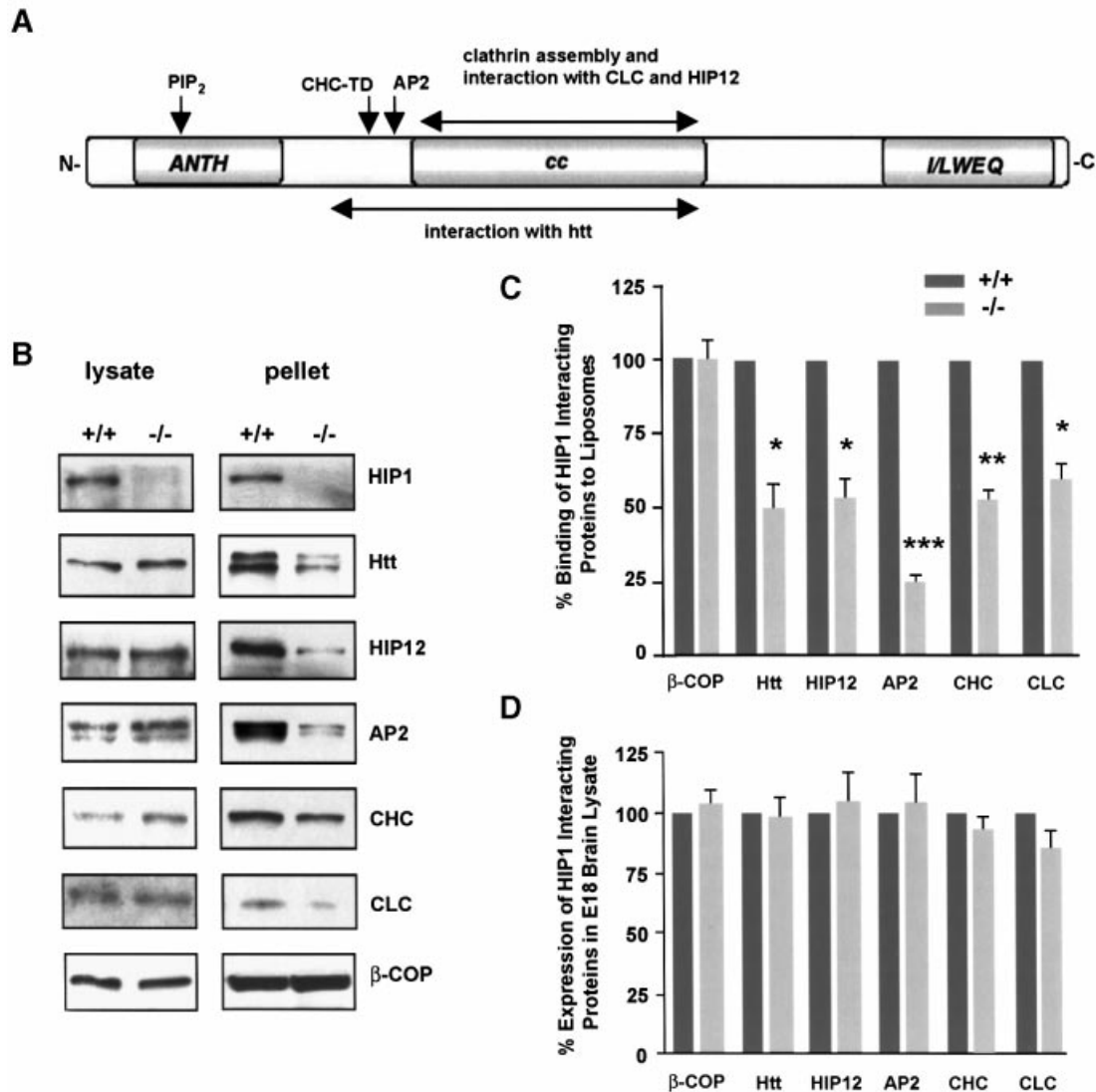


Fig. 5. The recruitment of endocytic proteins to liposomal membranes is decreased in brain lysate of $HIP1^{-/-}$ mice. (A) Schematic of HIP1 protein domains and sites of protein and phospholipid interaction. (B) Liposomal binding of endocytic proteins in brain lysates of wild-type (+/+) and homozygous (-/-) E18 embryos was analyzed by western blot. (C) The amount of bound protein in brain lysates from $HIP1^{-/-}$ mice compared with wild type was determined by densitometry ($n = 3$, * $P < 0.05$, ** $P < 0.005$, *** $P < 0.0005$ by t -test). (D) Expression of endocytic proteins in brain lysate of E18 wild-type (+/+) and $HIP1^{-/-}$ embryos was analyzed by western blot and quantified by densitometry. Results represent the percentage of expressed protein in $HIP1^{-/-}$ mouse brain lysate relative to wild type ($n = 3$).

dendrites in immature neurons after 6 days *in vitro* (6 DIV; Figure 6, top). The expression of HIP1 is greater in dendrites where there is limited colocalization with synaptotagmin an abundant protein associated with presynaptic vesicles. Similarly, no colocalization between HIP1 and synaptotagmin or the synaptic vesicle marker synaptophysin is evident in dendrites of more mature neurons at 16 DIV following incubation with either the monoclonal antibody (mAb) HIP1#9 or polyclonal antibody (pAb) HIP1FP against HIP1 (Figure 6). Again immunolocalization of HIP1 is strongest in the somato-dendritic compartment and prominent in cell bodies. In summary, cultured neurons reveal abundant levels of HIP1 in the dendritic compartment, which suggests its involvement in postsynaptic clathrin-mediated endocytic events.

HIP1 partially colocalizes with GluR1 and redistributes following AMPA stimulation

AMPA-type glutamate receptors are targets of constitutive and regulated clathrin-mediated endocytosis in primary hippocampal neurons (Carroll *et al.*, 1999; Lin *et al.*, 2000; Man *et al.*, 2000). Following treatment with either glutamate or AMPA the majority of GluR1-containing AMPA receptors are internalized and accumulate in early endosomal structures and cell bodies (Lissin *et al.*, 1999; Ehlers, 2000; Lin *et al.*, 2000). To investigate the role of HIP1 in AMPA receptor internalization, we first analyzed whether HIP1 colocalizes with AMPA receptors in primary hippocampal neurons. Confocal images of HIP1 immunostaining are punctate and show extensive colocalization with GluR1 in dendrites and in cell bodies

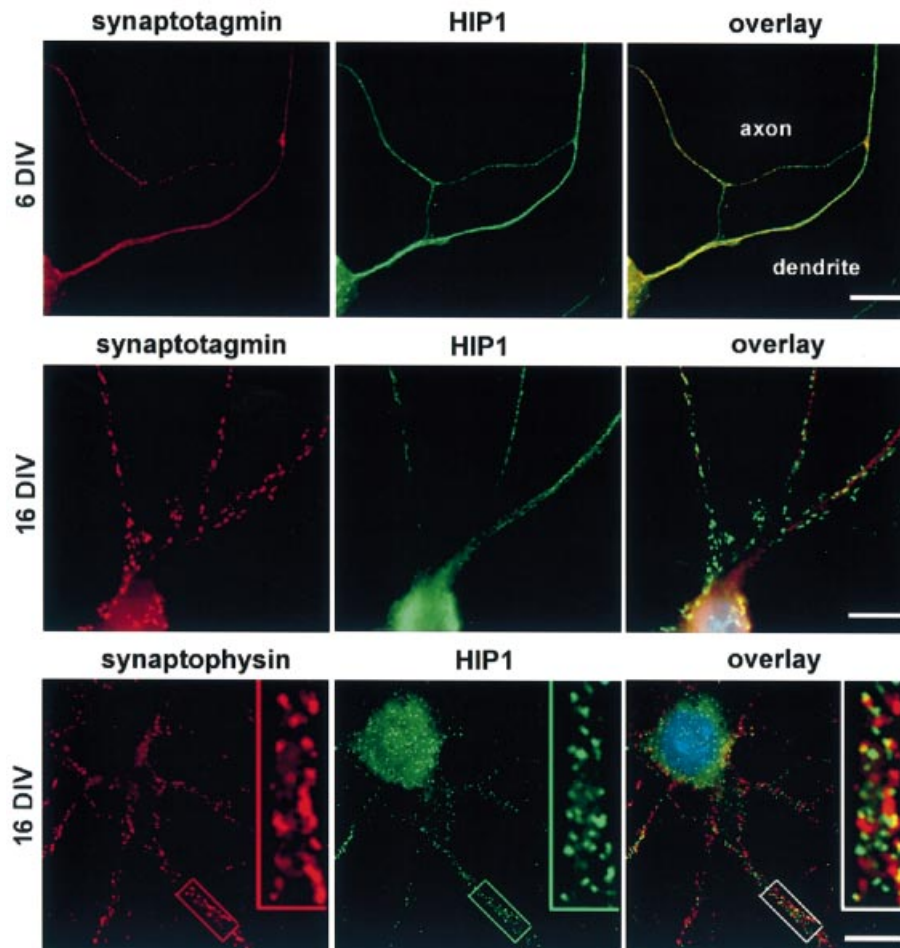


Fig. 6. HIP1 is expressed in the somatodendritic compartment in primary hippocampal neurons. HIP1 expression was analyzed by double immunofluorescence in primary hippocampal neurons after 6–21 days in culture. Synaptotagmin and synaptophysin immunolabeling is shown in red. HIP1 immunostaining was either detected with the mAb HIP1#9 (top and middle) or the pAb HIP1FP (bottom) and is shown in green. HIP1 does not colocalize with synaptic vesicle markers and shows a greater enrichment in the somatodendritic compartment. Nuclei were counterstained with DAPI shown in the electronic overlays (in blue). Scale bar = 10 μ M.

(Figure 7A). Interestingly, bath application with 100 μ M AMPA led to a redistribution of both GluR1-containing AMPA receptors and HIP1 from dendrites and consequent concentration in neuronal cell bodies (Figure 7B). This, together with the colocalization of HIP1 and GluR1, suggests that HIP1 might be involved in the relocation of AMPA receptors following AMPA-receptor stimulation through its function in clathrin-mediated endocytosis. To explore this hypothesis, we analyzed whether GluR1-containing AMPA receptors and HIP1 colocalize in the same endocytic compartment. Extensive colocalization of GluR1, HIP1 and the early endosomal marker EEA1 was observed after AMPA receptor stimulation for 5 min. Furthermore, pull-down experiments with a GST fusion protein encompassing amino acids (aa) 199–614 of HIP1, (HIP1-199–614), demonstrate an interaction of HIP1 with GluR1 (Chopra *et al.*, 2000; Figure 7D). This interaction could be mediated through binding to AP2 since both GluR1 and HIP1 associate with AP2 (Figure 7D; Metzler *et al.*, 2001; Lee *et al.*, 2002). Taken together, our data suggest that HIP1 is required for normal AMPA receptor trafficking. To test this further, we analyzed whether

ligand-induced AMPA receptor internalization is altered in neurons of HIP1^{-/-} mice.

Internalization of GluR1-containing AMPA receptors is abolished in HIP1^{-/-} mice

The effects of HIP1 on ligand-induced AMPA-receptor internalization were determined using a quantitative colorimetric assay that measures changes in the cell surface expression of AMPA receptors in unstimulated and stimulated cells (Figure 8A; Man *et al.*, 2000). This assay is based on the differential recognition of cell surface receptors and the total receptor pool under non-permeant and permeant conditions, respectively. Cortical neurons were treated with 100 μ M AMPA for 10 min or left untreated and the resulting change in the percentage of cell surface-expressed GluR2-containing AMPA receptors was determined for each genotype. In unstimulated neurons, ~60% of GluR2-containing AMPA receptors are expressed on the cell surface. This percentage is reduced to 37% following AMPA stimulation. In contrast, surface expression of GluR2 in neurons from HIP1^{-/-} mice remained constant suggesting a block in AMPA receptor

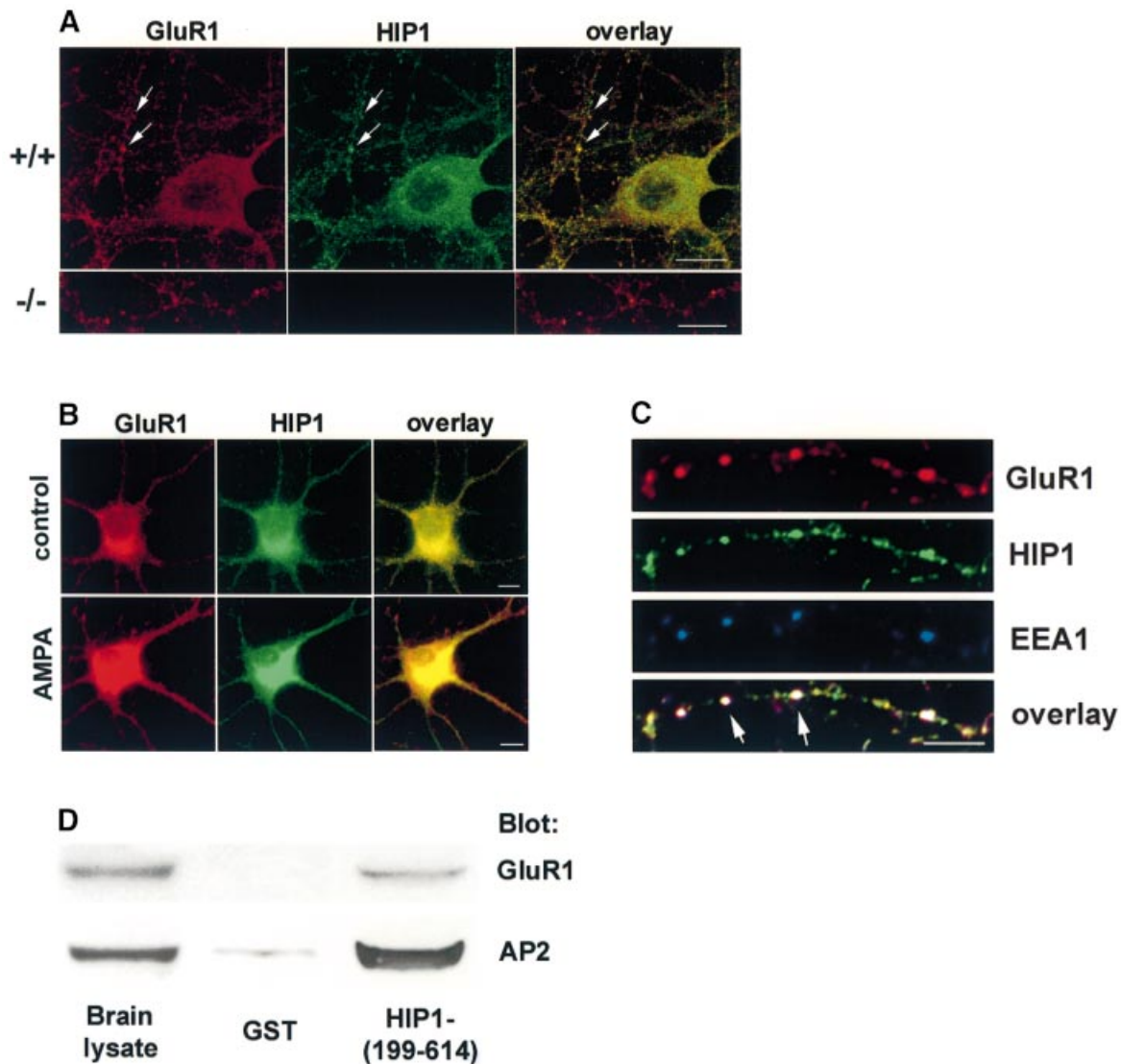


Fig. 7. HIP1 colocalizes and interacts with GluR1. **(A)** Expression of GluR1 (in red) and HIP1 (in green) was analyzed by double immunofluorescence in primary hippocampal neurons from wild-type (top) and HIP1^{-/-} littermates (bottom) after 15 DIV. Confocal images demonstrate extensive colocalization of HIP1 and GluR1 in dendrites and cell bodies (see arrows). No specific immunolabeling for HIP1 was detected in neurons derived from HIP1^{-/-} mice. Scale bar = 10 μM. **(B)** Stimulation of hippocampal neurons with 100 μM AMPA for 10 min leads to relocation of GluR1 (in red) and HIP1 (in green) and enrichment in cell bodies compared with control cultures. Scale bar = 10 μM. **(C)** GluR1 (in red), HIP1 (in green) and EEA1 (in blue) colocalize (see arrows) in primary hippocampal neurons stimulated with 100 μM AMPA for 5 min. Scale bar = 10 μM. **(D)** Soluble proteins from brain extracts were affinity-purified with equal amounts of either GST alone or a GST fusion protein encoding a fragment of HIP1 bound to glutathione-Sepharose beads. Proteins specifically bound to the beads were analyzed by western blot with anti-GluR1 and anti-AP2 Abs as indicated.

internalization. This effect is not generalized since constitutive transferrin receptor trafficking was normal in HIP1^{-/-} mice.

The colorimetric assay measures the net change in cell surface receptor expression that results from receptor internalization and receptor insertion. To obtain a more accurate measure of receptor internalization, we studied the effect of HIP1 on ligand-induced AMPA receptor internalization based on a quantitative fluorescent internalization assay (Lin *et al.*, 2000). This assay allows determination of the percentage ratio between pre-labeled cell surface (in green) and internalized (in red) GluR1 receptors with or without stimulation.

Hippocampal neurons were challenged with 100 μM glutamate for 10 min and the resulting internalization of

AMPA receptor-containing GluR1 subunits was determined (Figure 8C and D). Under control conditions (saline alone) wild-type neurons showed little constitutive GluR1 internalization, as indicated by the weak red staining. However, wild-type neurons showed a dramatic increase in GluR1 internalization after glutamate treatment, as the intensity of green cell surface staining decreased while the intensity of red staining in cell bodies increased. Again, this effect was markedly inhibited in HIP1^{-/-} neurons where most of the staining remained associated with cell surface-expressed GluR1 receptors after glutamate stimulation, similar to cultures exposed to salt solution alone (control). Quantification of this result showed a highly significant difference in response to glutamate for HIP1^{-/-} neurons ($n = 3$ independent experiments, $P < 0.01$

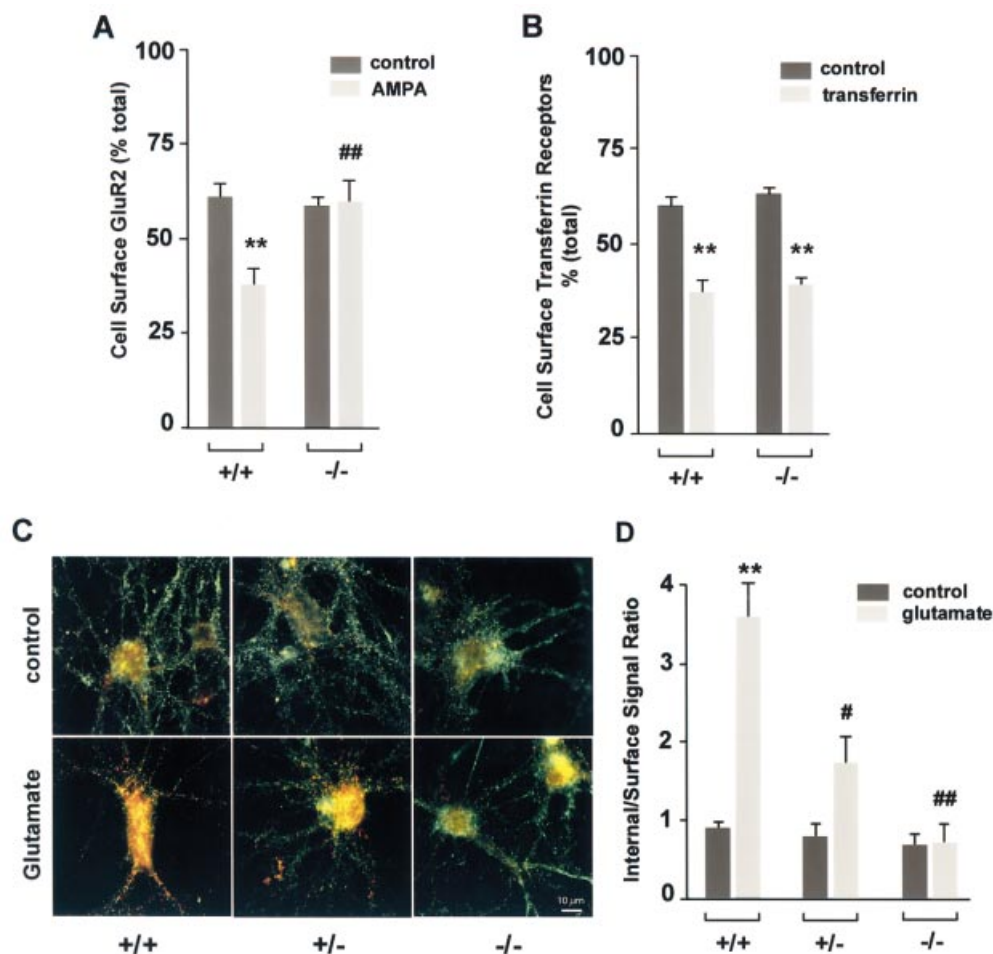


Fig. 8. AMPA receptor internalization is decreased in primary neurons of $HIP1^{-/-}$ mice. (A) Cortical neurons were established from wild-type (+/+) and homozygous (-/-) littermates. After 12–15 DIV the percentage of surface-expressed GluR2 was determined in a quantitative colorimetric assay in control and 100 μ M AMPA-stimulated cultures under non-permeant and permeant conditions. (B) As in (A), the percentage of surface-expressed transferrin receptor was determined in a quantitative colorimetric assay in control and in cultures treated with 2 mg/ml apo-transferrin under non-permeant and permeant conditions. (C) Hippocampal neurons cultured from wild-type (+/+), heterozygous (+/-) and homozygous (-/-) littermates were first labeled with an Ab recognizing an extracellular epitope of GluR1, followed by treatment with either control solution (medium alone) or 100 μ M glutamate for 10 min at 37°C. Surface GluR1 was then visualized using a green secondary Ab, whereas internalized GluR1 was labeled with a red secondary Ab. (D) Internalization was quantified as the red-to-green signal ratio, which represents the ratio of the internalized GluR1 to the GluR1 remaining on the cell surface after different treatments (see Materials and methods). Red-to-green ratios were averaged for each group in each of three different experiments (using three different batches of cultures). ** $P < 0.01$ for within genotype, between treatment comparison; # $P < 0.05$ or ## $P < 0.01$ for within treatment, between genotype comparison.

compared with wild type) demonstrating that glutamate-stimulated GluR1 internalization is blocked in neurons from $HIP1^{-/-}$ mice. Moreover, this effect is dose-dependent since only modest internalization was observed in $HIP1^{+/-}$ neurons (Figure 8D; $n = 3$, $P < 0.05$ compared with wild-type).

Discussion

HIP1 functions in clathrin-mediated endocytosis

In this study, we have demonstrated that the endocytic protein *HIP1* is essential for glutamate-evoked clathrin-mediated endocytosis of GluR1-containing AMPA receptors in hippocampal neurons. Furthermore, we have shown that the defect in clathrin-mediated endocytosis in $HIP1^{-/-}$ mice is associated with a severe progressive neurological phenotype characterized by wasting, tremor, gait ataxia and a thoracolumbar kyphosis.

HIP1 recruits endocytic proteins, such as clathrin and AP2, to liposomal membranes, which are decreased in brain extracts of mice lacking *HIP1*. This function is performed through an N-terminal fragment (aa 1–533), containing the ANTH domain and binding sites for clathrin and AP2, which recruits these proteins to Ptd-Ins(4,5) P_2 -containing membranes (see Figure 5; Mishra *et al.*, 2001). Further evidence for *HIP1* function in clathrin-mediated endocytosis comes from internalization studies of AMPA receptors. The internalization of AMPA receptors can be triggered by activation of AMPA, *N*-methyl-D-aspartate (NMDA), metabotropic glutamate or insulin receptors and is a well-established model for studying clathrin-mediated endocytosis (Lin *et al.*, 2000; Man *et al.*, 2000; Snyder *et al.*, 2001; Malinow and Malenka, 2002). We observed that the internalization of GluR1-containing AMPA receptors was completely abolished in neurons of $HIP1^{-/-}$ mice following AMPA

receptor activation. Remarkably, this defect is not compensated for by its family member, namely HIP12. One explanation for the lack of redundancy in function by HIP12 is that HIP1 expression in brain tissue is highest during embryogenesis and early postnatal life and subsequently declines, while expression of HIP12 is low during early brain development and increases postnatally (Legendre-Guillemain *et al.*, 2002).

HIP1 is required for internalization of GluR1-containing AMPA receptors

Expression analyses of HIP1 revealed limited colocalization with synaptic vesicle proteins. While some HIP1 can be detected in axons, it is unclear whether it plays any functional role at presynaptic nerve terminals. Defects in presynaptic structure and/or function occur following targeted inactivation of several endocytic proteins such as α -adaptin, AP180, endophilin, synaptojanin and amphiphysin (Gonzalez-Gaitan and Jackle, 1997; Zhang *et al.*, 1998; Cremona *et al.*, 1999; Di Paolo *et al.*, 2002; Verstreken *et al.*, 2002). Indeed, we did not observe any gross alterations in neurotransmission, or morphological changes in mutant synapses by electron microscopy (Supplementary data 2). Instead, the immunocytochemistry data suggests that a large portion of HIP1 is abundant in the somatodendritic compartment.

HIP1 partially colocalizes with AMPA receptors and this colocalization raised the possibility of a functional interaction between these proteins. This was supported by the observed defect in AMPA but not transferrin receptor endocytosis in primary neurons from HIP1^{-/-} mice suggesting a cargo-specific role of HIP1 in clathrin-mediated endocytosis. Several other endocytic proteins have recently emerged as cargo-specific adaptors apart from AP2 (Ohno *et al.*, 1995). For example, β -arrestin is a monomeric adaptor that binds to activated G-protein coupled receptors and mediates their desensitization through recruitment of the endocytic machinery; AP180 regulates synaptic vesicle size and was shown recently to regulate the abundance of GluR1 receptors at postsynaptic elements in *Caenorhabditis elegans*, and disabled-2 targets LDL receptors for endocytosis (Miller and Lefkowitz, 2001; Burbea *et al.*, 2002; Mishra *et al.*, 2002). All these proteins, including HIP1, regulate the surface expression of specific proteins and have the ability to recruit the endocytic machinery to sites of endocytosis.

Interestingly, HIP1 not only regulates trafficking of AMPA receptors but AMPA receptor stimulation also influences localization of HIP1. Previous reports have shown that GluR1-containing AMPA receptors enter an endosomal compartment following AMPA stimulation (Ehlers, 2000). In fact, the observed colocalization of GluR1 and HIP1 following AMPA stimulation in early endosomes suggests that HIP1 remains associated with AMPA receptors in a complex following their internalization and enters the same endosomal compartment. This is further supported by the observation that GluR1 and HIP1 can physically interact. The recent finding that ANTH/ENTH-domain-containing proteins, including HIP1, bind to tubulin provides a potential link to retrograde transport pathways along microtubules (Hussain *et al.*, 2003). This concept is also attractive from the point of view that HIP1 interacts with huntingtin which localizes to vesicles and

microtubules and interacts with huntingtin associating protein 1 (HAP1), which itself interacts with pGlued and hrs; proteins involved in transport along microtubules and trafficking from endosomes to lysosomes (X.J.Li *et al.*, 1995, S.H.Li *et al.*, 1998, Y.Li *et al.*, 2002). These findings suggest that HIP1 may not only influence the internalization of AMPA receptors but also provide links to the intracellular transport machinery that enables sorting and degradation of AMPA receptors.

The phenotypic effects of HIP1 deficiency

Mice lacking HIP1 develop a phenotype that originates in the CNS characterized by wasting, tremor and a gait ataxia secondary to a rigid thoracolumbar kyphosis. This phenotype correlates with changes in the trafficking of AMPA receptor subunits. However, the precise mechanism by which the defect in AMPA receptor trafficking leads to the observed phenotype is not yet clear.

An increase in the residency time of cell surface GluR1 resulting from altered trafficking may influence the net influx of Ca²⁺ through these receptors. This is probably of greater consequence during development as the vast majority of cells in the adult CNS express Ca²⁺-impermeable AMPA receptors, while unique patterns of ionotropic glutamate receptors are expressed during development (Martin *et al.*, 1998). Ca²⁺-permeable AMPA receptors are important in mediating growth-cone movement, synaptogenesis, dendritic architecture and the formation of neuronal circuitry (Tanaka *et al.*, 2000; Inglis *et al.*, 2002). Moreover, the high level of HIP1 expression in embryonic and early prenatal brain argues for an important role of HIP1 in development.

We have shown that HIP1 influences AMPA receptor endocytosis, but it is possible that HIP1 controls the internalization of other glutamate and non-glutamate receptors with consequent effects on their activity. For instance, activation of extrasynaptic NMDA receptors promotes apoptotic pathways and it remains to be determined whether HIP1 could also alter NMDA receptor function by influencing their endocytosis (Hardingham *et al.*, 2002). HIP1 has already been linked to apoptotic pathways through its pseudo death-effector domain and its interaction with another pseudo death-effector-containing protein, HIP1 protein interactor (HIPPI), that leads to caspase 8 recruitment and the activation of the cell death machinery *in vitro* (Gervais *et al.*, 2002).

The immature basal ganglia and motor cortex are especially vulnerable to excitotoxicity, leading to a variety of defects later in life including wasting, ataxia, tremor and skeletal deformities (Johnston, 1997). This vulnerability may be related to receptor overstimulation and changes in neuronal circuitry, and it is conceivable that alterations in glutamate and non-glutamate receptor surface expression in early brain development resulting from lack of HIP1 contributes to the phenotypic effects seen in the HIP1^{-/-} mice. Our observation that no gross changes in volume or neuronal counts were evident in the hippocampus of HIP1^{-/-} mice ($n = 2$) does not rule out that less-obvious changes in cell numbers, neuronal architecture or inter-neuronal connectivity may be present. In summary, we have shown that HIP1 is crucial for AMPA receptor trafficking in the CNS and that these deficits are associated with major progressive neurological deficits.

Materials and methods

HIP1 gene targeting

See Supplementary data 1 for a detailed description of HIP1 gene targeting. Correctly targeted ES cell clones were microinjected into C57/B16 blastocysts and implanted into pseudopregnant females to produce chimeras (Metzler *et al.*, 1994). Chimeras were bred with C57/B16 females and F1 heterozygous mice were intercrossed to generate the F2 generation. Wild-type, hetero- and homozygous mice were identified by PCR and Southern blot analysis. The characterization of HIP1^{-/-} mice was performed on a mixed background of 129/SvJ × C57/B16 with mice from line 3 and 4.

Expression analyses by western blot and LacZ staining

The following Abs were used for expression analyses by western blot as described previously (Metzler *et al.*, 2001): the mouse mAb HIP1 #9 and the rabbit pAb against HIP12 (HIP12FP) were described previously (Chopra *et al.*, 2000; Metzler *et al.*, 2001); mouse mAbs recognizing α -adaplin and CHC were from BD Transduction Laboratories; mouse mAb recognizing CLC was from Covance, CA; the mouse mAb against β -COP was from Affinity Bio Reagents, CO; the mAb against GAPDH was from Chemicon International, CA; and the anti-actin Ab from Sigma, MO.

LacZ expression analyses of brain and spinal cord sections were performed as described previously (Lobe *et al.*, 1999).

Footprint analysis

A paper-lined runway (75 × 10 × 15 cm) was used for the analysis. Each mouse was permitted to familiarize itself with the area for ~2 min, then its paws were painted with non-toxic paint (Pro-Art, Beaverton, USA); the animal was returned to one end of the runway and allowed to walk normally to the far end. Measurements of stride length and stride width were averaged over six consecutive prints for each mouse.

Kaplan–Meier and statistical analyses

The percentage of mice with thoracolumbar kyphosis and neurological abnormalities was determined by Kaplan–Meier analyses. To determine significant differences between the onset of the thoracolumbar kyphosis in male and female mice, χ^2 analysis was performed. All other statistical analyses were performed by Student's *t*-test.

X-ray analysis and Alzarin Red stain of bone

Mice were sacrificed and exposed to a Faxitron X-ray machine at 50 V for 17 s. Subsequently, mice were skinned and eviscerated and transferred into a 0.1% KOH solution for 1 week. The solution was replaced and Alzarin Red S (Aldrich) was added to a final concentration of 0.015%. Skeletons were incubated for another week and transferred into glycerol.

Nerve conduction and EMG analysis

Mice were anesthetized with ketamine (140 mg/kg) and xylazine (15 mg/kg). Nerve conduction and EMG were performed using a Nicolet Viking EMG machine. For stimulation, two monopolar EMG electrodes were placed across the sciatic notch. The CMAP response was recorded from the gastrocnemius muscle using a third monopolar EMG electrode. The reference was placed in the foot. The ground electrode, a fifth monopolar electrode, was placed at the ankle. A supramaximal response was obtained by gradually increasing the stimulus strength until no further increase in CMAP amplitude was obtained. Signals were amplified and bandpass filtered (2–10 KHz).

Liposome binding and GST pull-down

Heterozygous matings were set up and embryonic brains were isolated from pregnant females at E18.5. Ten brains of each genotype were pooled and homogenized in 10 mM HEPES–KOH pH 7.4, 0.83 mM benzamidine, 0.25 mM PMSF, 0.5 μ g/ml aprotinin and 0.5 μ g/ml leupeptin. After preclearing at 800 g for 5 min at 4°C the supernatant was ultracentrifuged at 205 000 g and processed as described previously (Takei *et al.*, 1996).

GST pull-down experiments were carried out as described previously (Metzler *et al.*, 2001).

Immunofluorescence

Hippocampal neurons were established from newborn mice and cultured as described previously (Lin *et al.*, 2000). After 15 DIV, neurons were treated with 100 μ M AMPA for 5 or 10 min at 37°C or left untreated. Neurons were then washed in ice-cold PBS, fixed in 4% paraformaldehyde (PFA) in PBS, and permeabilized in 0.3% Triton X-100, 1% PFA.

Non-specific binding sites were blocked by incubation with 3% normal goat serum (NGS) in PBS. For double immunofluorescence, cells were incubated with mAb HIP1#9 or the pAb HIP1FP (Chopra *et al.*, 2000) in 2% NGS in PBS at 4°C overnight followed by incubation with secondary Abs directed against synaptotagmin, synaptophysin (both from BD Transduction Laboratories), EEA1 (Santa Cruz, CA) or GluR1 (Upstate Biotechnology, NY), respectively, for 2 h at room temperature with extensive washing in PBS, 1% BSA between each incubation. Neurons were then incubated with Alexa 488-, 546-, 596- or 633-labeled secondary antibodies (Molecular Probes), washed, mounted and analyzed by conventional or confocal microscopy.

Colorimetric assay

The same density of cortical neurons were treated with 100 μ M AMPA for 10 min, or 2 mg/ml apo-transferrin (Sigma) for 30 min at 37°C, then fixed in 4% PFA/4% sucrose for 10 min. Half of the cells in each group were then permeabilized with 0.1% Triton X-100 for 5 min. Cells were incubated with either a mAb against the extracellular domain of GluR2 (Chemicon) or a pAb against the extracellular domain of the transferrin receptor (Santa Cruz) to label surface-expressed receptors under non-permeant conditions or the entire receptor pool under permeant conditions as described previously (Man *et al.*, 2000). Values for each group were averaged using at least three separate plates from three independent cell cultures.

Internalization assay

Live hippocampal neurons of 13–15 DIV were incubated for 15 min at 37°C with an Ab directed against an extracellular region of GluR1 (5 μ g/ml; Oncogene Research Products, MA). Neurons were then washed with PBS/2 mM MgCl₂/0.1 mM CaCl₂, followed by treatment for 10 min at 37°C with either conditioned growth medium containing 100 μ M glutamate and 1 μ M TTX (glutamate), or conditioned growth medium containing TTX only (control). This challenge with glutamate is not expected to appreciably activate NMDA receptors because of the presence of 0.8 mM Mg²⁺ in the medium and the fact that AMPA receptor-mediated membrane depolarization would be brief (ms) due to receptor depolarization. Neurons were then fixed for 15 min with 4% PFA/4% sucrose in PBS without permeabilization and incubated with Alexa-488-labeled secondary Ab for 1 h at room temperature to visualize surface GluR1s. Then neurons were permeabilized for 1 min with 100% methanol at –20°C and treated with Cy3-labeled secondary Abs (donkey anti-rabbit; Jackson ImmunoResearch Laboratories, PA) for 1 h at room temperature to recognize pre-labeled internalized GluR1s. Images were acquired using a CCD camera and fluorescence intensities at both somatic and dendritic areas were measured using IDL software (Research Systems Inc., CO; Prange and Murphy, 2001) and quantified as red-to-green signal ratio to determine the degree of internalization. The regions of interest were chosen on superimposed gray scale pictures and then measured by the program for signal intensities from both green and red channels and the red-to-green ratios were calculated automatically. Background values near the areas of interest were also measured and subtracted. About 60 regions of interest were measured for each sample. The values of the red-to-green ratio were averaged for each group in each experiment.

Supplementary data

Supplementary data are available at *The EMBO Journal* Online.

Acknowledgements

The pIFS promoter-trap vector was kindly provided by L.Lefebvre. We thank Dr Timothy A.Ryan for his help with electrophysiological studies and Yu-Zhou Yang, Anita Borowski, Nagat Bissada, Kuljeet Vaid and Lisa Bertram for technical support. This work is supported by the CDGN and by the Canadian Institutes of Health Research (CIHR) grant MT-9133 to M.R.H. and grant MT-12699 to L.A.R. Further support was provided by Merck-Frosst Canada to M.R.H. and M.M. J.G. was supported by a CNRP (Canadian Neurotrauma Research Program) Fellowship offered through CIHR. R.S.D. is supported by a Wellcome Travelling Research Fellowship. V.L.-G. is a CIHR postdoctoral fellow. P.S.M., L.A.R. and Y.T.W. are CIHR investigators. M.R.H. is a holder of a Canada Research Chair in Human Genetics.

References

- Ahle, S., Mann, A., Eichelsbacher, U. and Ungewickell, E. (1988) Structural relationships between clathrin assembly proteins from the Golgi and the plasma membrane. *EMBO J.*, **7**, 919–929.
- Brodsky, F.M., Chen, C.Y., Kneuhl, C., Towler, M.C. and Wakeham, D.E. (2001) Biological basket weaving: formation and function of clathrin-coated vesicles. *Annu. Rev. Cell. Dev. Biol.*, **17**, 517–568.
- Buckley, K.M., Melikian, H.E., Provoda, C.J. and Waring, M.T. (2000) Regulation of neuronal function by protein trafficking: a role for the endosomal pathway. *J. Physiol.*, **525**, 11–19.
- Burbea, M., Dreier, L., Dittman, J.S., Grunwald, M.E. and Kaplan, J.M. (2002) Ubiquitin and AP180 regulate the abundance of GLR-1 glutamate receptors at postsynaptic elements in *C. elegans*. *Neuron*, **35**, 107–120.
- Carroll, R.C., Beattie, E.C., Xia, H., Luscher, C., Altschuler, Y., Nicoll, R.A., Malenka, R.C. and Von Zastrow, M. (1999) Dynamin-dependent endocytosis of ionotropic glutamate receptors. *Proc. Natl Acad. Sci. USA*, **96**, 14112–14117.
- Chopra, V.S. *et al.* (2000) HIP12 is a non-proapoptotic member of a gene family including HIP1, an interacting protein with huntingtin. *Mamm. Genome*, **11**, 1006–1015.
- Cremona, O. *et al.* (1999) Essential role of phosphoinositide metabolism in synaptic vesicle recycling. *Cell*, **99**, 179–188.
- De Camilli, P., Slepnev, V.I., Shupliakov, O. and Brodin, L. (2001) Synaptic vesicle endocytosis. In Cowan, W.M., Sudhof, T.C., Stevens, C.F. and Davies, K. (eds), *Synapse*. The Johns Hopkins University Press, Baltimore, MD, pp. 217–274.
- DiFiglia, M. *et al.* (1995) Huntingtin is a cytoplasmic protein associated with vesicles in human and rat brain neurons. *Neuron*, **14**, 1075–1081.
- Di Paolo, G. *et al.* (2002). Decreased synaptic vesicle recycling efficiency and cognitive deficits in amphiphysin 1 knockout mice. *Neuron*, **33**, 789–804.
- Ehlers, M.D. (2000) Reinsertion or degradation of AMPA receptors determined by activity-dependent endocytic sorting. *Neuron*, **28**, 511–525.
- Faber, P.W., Barnes, G.T., Srinidhi, J., Chen, J., Gusella, J.F. and MacDonald, M.E. (1998) Huntingtin interacts with a family of WW domain proteins. *Hum. Mol. Genet.*, **7**, 1463–1474.
- Ford, M.G., Pearce, B.M., Higgins, M.K., Vallis, Y., Owen, D.J., Gibson, A., Hopkins, C.R., Evans, P.R. and McMahon, H.T. (2001) Simultaneous binding of PtdIns_{4,5}P₂ and clathrin by AP180 in the nucleation of clathrin lattices on membranes. *Science*, **291**, 1051–1055.
- Ford, M.G., Mills, I.G., Peter, B.J., Vallis, Y., Praefcke, G.J., Evans, P.R. and McMahon, H.T. (2002) Curvature of clathrin-coated pits driven by epsin. *Nature*, **419**, 361–366.
- Gervais, F.G. *et al.* (2002) Recruitment and activation of caspase-8 by the Huntingtin-interacting protein Hip-1 and a novel partner Hipp1. *Nat. Cell Biol.*, **4**, 95–105.
- Gonzalez-Gaitan, M. and Jackle, H. (1997) Role of *Drosophila* α -adaptin in presynaptic vesicle recycling. *Cell*, **88**, 767–776.
- Hao, W., Luo, Z., Zheng, L., Prasad, K. and Lafer, E.M. (1999) AP180 and AP-2 interact directly in a complex that cooperatively assembles clathrin. *J. Biol. Chem.*, **274**, 22785–22794.
- Hardingham, G.E., Fukunaga, Y. and Bading, H. (2002) Extrasynaptic NMDARs oppose synaptic NMDARs by triggering CREB shut-off and cell death pathways. *Nat. Neurosci.*, **5**, 405–414.
- Hussain, N.K., Yamabhai, M., Bhakar, A.L., Metzler, M., Ferguson, S.S.G., Hayden, M.R., McPherson, P.S. and Kay, B.K. (2003) A role for ENTH/ANTH domains in tubulin binding. *J. Biol. Chem.*, submitted.
- Inglis, F.M., Crockett, R., Korada, S., Abraham, W.C., Hollmann, M. and Kalb, R.G. (2002) The AMPA receptor subunit GluR1 regulates dendritic architecture of motor neurons. *J. Neurosci.*, **22**, 8042–8051.
- Itoh, T., Koshiba, S., Kigawa, T., Kikuchi, A., Yokoyama, S. and Takenawa, T. (2001) Role of the ENTH domain in phosphatidylinositol-4,5-bisphosphate binding and endocytosis. *Science*, **291**, 1047–1051.
- Johnston, M.V. (1997) Hypoxic and ischemic disorders of infants and children. Lecture for 38th meeting of Japanese Society of Child Neurology, Tokyo, Japan, July 1996. *Brain Dev.*, **19**, 235–239.
- Kalchman, M.A. *et al.* (1997) HIP1, a human homologue of *S.cerevisiae* Sla2p, interacts with membrane-associated huntingtin in the brain. *Nat. Genet.*, **16**, 44–53.
- Lee, S.H., Liu, L., Wang, Y.T. and Sheng, M. (2002) Clathrin adaptor AP2 and NSF interact with overlapping sites of GluR2 and play distinct roles in AMPA receptor trafficking and hippocampal LTD. *Neuron*, **36**, 661–674.
- Legendre-Guillemin, V., Metzler, M., Charbonneau, M., Gan, L., Chopra, V., Philie, J., Hayden, M.R. and McPherson, P.S. (2002) HIP1 and HIP12 display differential binding to F-actin, AP2, and clathrin. Identification of a novel interaction with clathrin light chain. *J. Biol. Chem.*, **277**, 19897–19904.
- Li, S.H., Gutekunst, C.A., Hersch, S.M. and Li, X.J. (1998) Interaction of huntingtin-associated protein with dynactin P150^{Glued}. *J. Neurosci.*, **18**, 1261–1269.
- Li, X.J., Li, S.H., Sharp, A.H., Nucifora, F.C., Jr., Schilling, G., Lanahan, A., Worley, P., Snyder, S.H. and Ross, C.A. (1995) A huntingtin-associated protein enriched in brain with implications for pathology. *Nature*, **378**, 398–402.
- Li, Y., Chin, L.S., Levey, A.I. and Li, L. (2002) Huntingtin-associated protein 1 interacts with hepatocyte growth factor-regulated tyrosine kinase substrate and functions in endosomal trafficking. *J. Biol. Chem.*, **277**, 28212–28221.
- Lin, J.W., Ju, W., Foster, K., Lee, S.H., Ahmadian, G., Wyszynski, M., Wang, Y.T. and Sheng, M. (2000) Distinct molecular mechanisms and divergent endocytotic pathways of AMPA receptor internalization. *Nat. Neurosci.*, **3**, 1282–1290.
- Lissin, D.V., Carroll, R.C., Nicoll, R.A., Malenka, R.C. and Von Zastrow, M. (1999) Rapid, activation-induced redistribution of ionotropic glutamate receptors in cultured hippocampal neurons. *J. Neurosci.*, **19**, 1263–1272.
- Lobe, C.G., Koop, K.E., Kreppner, W., Lomeli, H., Gertsenstein, M. and Nagy, A. (1999) Z/AP, a double reporter for cre-mediated recombination. *Dev. Biol.*, **208**, 281–292.
- Malinow, R. and Malenka, R.C. (2002) AMPA receptor trafficking and synaptic plasticity. *Annu. Rev. Neurosci.*, **25**, 103–126.
- Man, H.Y., Lin, J.W., Ju, W.H., Ahmadian, G., Liu, L., Becker, L.E., Sheng, M. and Wang, Y.T. (2000) Regulation of AMPA receptor-mediated synaptic transmission by clathrin-dependent receptor internalization. *Neuron*, **25**, 649–662.
- Martin, L.J., Furuta, A. and Blackstone, C.D. (1998) AMPA receptor protein in developing rat brain: glutamate receptor-1 expression and localization change at regional, cellular, and subcellular levels with maturation. *Neuroscience*, **83**, 917–928.
- McPherson, P.S., Kay, B.K. and Hussain, N.K. (2001) Signaling on the endocytic pathway. *Traffic*, **2**, 375–384.
- Metzler, M., Gertz, A., Sarkar, M., Schachter, H., Schrader, J.W. and Marth, J.D. (1994) Complex asparagine-linked oligosaccharides are required for morphogenic events during post-implantation development. *EMBO J.*, **13**, 2056–2065.
- Metzler, M., Legendre-Guillemin, V., Gan, L., Chopra, V., Kwok, A., McPherson, P.S. and Hayden, M.R. (2001) HIP1 functions in clathrin-mediated endocytosis through binding to clathrin and adaptor protein 2. *J. Biol. Chem.*, **276**, 39271–39276.
- Miller, W.E. and Lefkowitz, R.J. (2001) Arrestins as signaling molecules involved in apoptotic pathways: a real eye opener. *Sci. STKE*, **2001**, E1.
- Mishra, S.K., Agostinelli, N.R., Brett, T.J., Mizukami, I., Ross, T.S. and Traub, L.M. (2001) Clathrin- and AP-2-binding sites in HIP1 uncover a general assembly role for endocytic accessory proteins. *J. Biol. Chem.*, **276**, 46230–46236.
- Mishra, S.K., Keyel, P.A., Hawryluk, M.J., Agostinelli, N.R., Watkins, S.C. and Traub, L.M. (2002) Disabled-2 exhibits the properties of a cargo-selective endocytic clathrin adaptor. *EMBO J.*, **21**, 4915–4926.
- Ohno, H. *et al.* (1995) Interaction of tyrosine-based sorting signals with clathrin-associated proteins. *Science*, **269**, 1872–1875.
- Prange, O. and Murphy, T.H. (2001) Modular transport of postsynaptic density-95 clusters and association with stable spine precursors during early development of cortical neurons. *J. Neurosci.*, **21**, 9325–9333.
- Roche, K.W., Standley, S., McCallum, J., Dune, L.C., Ehlers, M.D. and Wenthold, R.J. (2001) Molecular determinants of NMDA receptor internalization. *Nat. Neurosci.*, **4**, 794–802.
- Rosenthal, J.A., Chen, H., Slepnev, V.I., Pellegrini, L., Salcini, A.E., Di Fiore, P.P. and De Camilli, P. (1999) The epsins define a family of proteins that interact with components of the clathrin coat and contain a new protein module. *J. Biol. Chem.*, **274**, 33959–33965.
- Sheng, M. and Kim, M.J. (2002) Postsynaptic signaling and plasticity mechanisms. *Science*, **298**, 776–780.
- Sittler, A., Walter, S., Wedemeyer, N., Hasenbank, R., Scherzinger, E., Eickhoff, H., Bates, G.P., Lehrach, H. and Wanker, E.E. (1998) SH3GL3 associates with the Huntingtin exon 1 protein and

- promotes the formation of polyglu-containing protein aggregates. *Mol. Cell*, **2**, 427–436.
- Snyder,E.M., Philpot,B.D., Huber,K.M., Dong,X., Fallon,J.R. and Bear,M.F. (2001) Internalization of ionotropic glutamate receptors in response to mGluR activation. *Nat. Neurosci.*, **4**, 1079–1085.
- Sun,J.Y., Wu,X.S. and Wu,L.G. (2002) Single and multiple vesicle fusion induce different rates of endocytosis at a central synapse. *Nature*, **417**, 555–559.
- Takei,K., Mundigl,O., Daniell,L. and De Camilli,P. (1996) The synaptic vesicle cycle: a single vesicle budding step involving clathrin and dynamin. *J. Cell Biol.*, **133**, 1237–1250.
- Tanaka,H., Grooms,S.Y., Bennett,M.V. and Zukin,R.S. (2000) The AMPAR subunit GluR2: still front and center-stage. *Brain Res.*, **886**, 190–207.
- Verstreken,P., Kjaerulff,O., Lloyd,T.E., Atkinson,R., Zhou,Y., Meinertzhagen,I.A. and Bellen,H.J. (2002) Endophilin mutations block clathrin-mediated endocytosis but not neurotransmitter release. *Cell*, **109**, 101–112.
- Waelter,S. *et al.* (2001) The huntingtin interacting protein HIP1 is a clathrin and α -adaptin-binding protein involved in receptor-mediated endocytosis. *Hum. Mol. Genet.*, **10**, 1807–1817.
- Wanker,E.E., Rovira,C., Scherzinger,E., Hasenbank,R., Walter,S., Tait,D., Colicelli,J. and Lehrach,H. (1997) HIP-I: a huntingtin interacting protein isolated by the yeast two-hybrid system. *Hum. Mol. Genet.*, **6**, 487–495.
- Zhang,B., Koh,Y.H., Beckstead,R.B., Budnik,V., Ganetzky,B. and Bellen,H.J. (1998) Synaptic vesicle size and number are regulated by a clathrin adaptor protein required for endocytosis. *Neuron*, **21**, 1465–1475.

*Received February 11, 2003; revised May 2, 2003;
accepted May 15, 2003*